J Sol-Gel Sci Technol (2011) 60:189–197
DOI 10.1007/s10971-011-2578-5

ORIGINAL PAPER

Formation of $Mg(OH)_2$ nanowhiskers on LTA zeolite surfaces using a sol–gel method

Junqiang Liu · Tae-Hyun Bae · Omoyemen Esekhile · Sankar Nair · Christopher W. Jones · William J. Koros

Received: 28 July 2011 / Accepted: 4 September 2011 / Published online: 20 September 2011

Abstract A facile three step sol–gel-precipitation process is used to synthesize $Mg(OH)_2$ nanowhiskers on micron-sized zeolite 5A particle surfaces at room temperature. The putative amorphous gelation product, $Mg(OH)_n(OR)_{2-n}$, forms first by a controlled hydrolysis and condensation reaction involving magnesium isopropoxide and water, ultimately leading to precipitation to form $Mg(OH)_2$ structures on the zeolite surface. The optimum conditions for one dimensional $Mg(OH)_2$ whisker formation are found to be six times the stoichiometric amount of water using 1 M HCl as the catalyst for the sol–gel reaction. The one-dimensional $Mg(OH)_2$ whiskers have an average diameter of 5–10 nm and length of 50–100 nm. The zeolite micropores are not affected by the $Mg(OH)_2$ whiskers formed on the surface. The surface roughened zeolite 5A, with a $Mg(OH)_2$ content of about 9 wt%, showed improved adhesion between the zeolite and the polymer in a mixed-matrix composite membrane.

Keywords Mixed matrix membrane · Grignard treatment · Sol–gel · Surface roughening

1 Introduction

The incorporation of zeolite particles into glassy polymer membranes to make mixed matrix membranes with enhanced separation performance is challenging because of a tendency for the formation of defective interfaces between the polymers and the zeolites [1–3]. Recently, a new method of mixed matrix membrane formation has been established and shown to be extendable to practical asymmetric fiber membranes. This method employs a Grignard treatment to modify the zeolite surface [4–6] and to improve the interfacial adhesion between the zeolite and the polymer, which is the most significant limitation facing widespread mixed matrix membrane application. The gas separation selectivity enhancement in mixed matrix dense films indicates improved interfacial adhesion, presumably by minimizing the entropic penalty for accommodating random coils of the polymer matrix in contact with the roughened surfaces of the molecular sieves.

The original Grignard treatment was intended to introduce methyl groups on the zeolite surface, making the solid hydrophobic, via reaction with methylmagnesium bromide. It was serendipitously found that a significant coating of $Mg(OH)_2$ was deposited on the zeolite particles as a result of the aqueous work-up used in the reaction. This $Mg(OH)_2$ coating resulted in a zeolite that adhered well to commercial poly(etherimide) used in membrane fabrication.

Subsequent investigation of the Grignard treatment method showed that the process involved growing $Mg(OH)_2$ whiskers on the zeolite surface in two steps. First dealumination products comprising NaCl and $AlCl_3$ were formed by $SOCl_2$ treatment of the aluminosilicate, with the latter proposed to act as nucleation sites for creation of $Mg(OH)_2$ whiskers on the surface [7]. Then methylmagnesium bromide was added to the mixture, followed by quenching in isopropanol, as shown in Eq. 1, to form magnesium isopropoxide and magnesium bromide [8, 9]. In previous reports, the $Mg(OH)_2$ was assumed to be formed by reaction between methylmagnesium bromide and water, as shown by Eq. 2 [4]. However, complete

J. Liu · T.-H. Bae · O. Esekhile · S. Nair · C. W. Jones · W. J. Koros (✉)
Georgia Institute of Technology, School of Chemical & Biomolecular Engineering, 311 Ferst Drive, Atlanta, GA 30332-0100, USA
e-mail: wjk@chbe.gatech.edu

elucidation of the reaction pathway was not achieved, and the original synthesis is somewhat difficult to control.

$$2CH_3MgBr + 2(CH_3)_2CHOH \rightarrow 2CH_4 + MgBr_2 + Mg(OCH(CH_3)_2)_2 \quad (1)$$

$$2CH_3MgBr + 2H_2O \rightarrow 2CH_4 + MgBr_2 + Mg(OH)_2 \quad (2)$$

In this work, we have reconsidered the reaction pathway in light of what is known about sol–gel chemistry of magnesium alkoxides, such as the species shown in Eq. 1. In addition, a streamlined, highly reproducible process has been developed that facillitates efficient coating of the zeolite crystals with $Mg(OH)_2$ nanostructures without the need for surface pretreatment.

2 Experimental

Zeolite 5A particles, with an average size of 2 μm, were purchased from Aldrich. Toluene (99.8% purity), tetrahydrofuran (THF 99.8% purity), isopropanol (99.5% purity), and methylmagnesium bromide (3.0 M solution in diethyl ether) were purchased from Aldrich and used without further purification. All chemicals were transferred into reactions vessels carefully through a syringe to avoid exposure to atmospheric moisture.

2.1 Synthesis of magnesium sol in the presence of zeolites

A mass of 8 g of zeolite 5A particles and a Teflon® coated magnetic stir bar were placed in a 200 mL reaction flask. All the particles and glassware were dried overnight at 150 °C in a vacuum oven. Then, 80 mL of toluene and 20 mL of methylmagnesium bromide were added into the sealed reaction flask. The dispersion was kept in a sonication bath (Branson 1510) overnight, before 80 mL of isopropanol were added slowly to react with the methylmagnesium bromide. The resulting milky sol dispersion product was divided into six 50 mL centrifuge vials.

2.2 Gelation of magnesium sol in the presence of zeolites

Water was then added into the vials of the sol dispersion dropwise. Sonication was used to assist the H_2O dispersion after addition of four drops of water, via a 55 W sonication horn (VCX130, Sonics) for 10 s. This process was repeated 5–10 times until the desired amount of water was added. The pH of the H_2O added was adjusted to 7.0, 1.0 and 0 by adding the appropriate amount of 35 wt% HCl solution into the de-ionized water. The resultant sol–gel dispersion was aged overnight without disruption.

2.3 Recovery of $Mg(OH)_2$ coated zeolites

The particles and reaction products were separated from the dispersion by a centrifuge. The supernatant was decanted and isopropanol was added to wash away the remaining toluene, with sonication at 55 W power for 30 s duration to assist the washing. This sonication and washing treatment was repeated three times. Zeolite particles were then centrifuged out of the isopropanol and water was then added, followed by sonication for three 30-second periods. The sonication and centrifuging procedures were repeated until the conductivity of the supernatant dropped below 30 μS m^{-1}. The final collected particles were dried overnight in a vacuum oven at 150 °C.

2.4 Mixed matrix membrane formation

A 25 wt% polymer dope was prepared with dried fluorinated polyimide 6FDA-DAM (Mw = 49,300) [10] and tetrahydrofuran (THF). The dope was rolled on a mixer overnight to dissolve the polymer. The treated or untreated zeolite molecular sieve particles were dried in a vacuum oven at 180 °C overnight, to remove moisture in the pores. A small amount of tetrahydrofuran was then added to the dried sieve in a 8 mL vial and a few bursts of sonication were applied to assist the dispersion of the sieve in THF. The polymer dope was then added to the sieves to achieve the desired particle-to-polymer ratio. The polymer-sieve dope was rolled and sonicated to assist the dispersion of sieves in the dope. The dopes were poured onto a glass plate, which was placed in a glove bag pre-saturated with THF vapor for at least 4 h. The dope was cast into the desired thickness (typically 30 micron) using a draw knife with appropriate specific clearance. The film was left in the glove bag overnight to let the THF solvent evaporate slowly. The film was further dried in a vacuum oven at 180 °C overnight to remove remaining solvent.

Butane isomer permeation tests on these films were done using a downstream-vacuum, pressure build up method, with an upstream pressure of 25 psi at 100 °C. The pressure decay method was used to measure the n-butane sorption capacity in the zeolite 5A micropores before and after surface treatments, using a method previously reported [10].

SEM images were obtained with a LEO 1550, equipped with a thermally assisted field emission gun operating at 5 kV. Elemental content was analyzed by Electron Dispersion Spectroscopy (EDS) measurements. Three measurements were done and an average was taken for each sample. Powder X-ray diffraction (XRD) patterns were obtained on a Philips X'pert diffractometer equipped with X'celerator using Cu Kα radiation.

3 Results and discussion

An efficient way to have the majority of Grignard reagent form $Mg(OH)_2$ is via first conversion of the Grignard to a magnesium alkoxide, followed by controlled hydrolysis and condensation of the magnesium sol.

Magnesium alkoxides have been widely used to synthesize $Mg(OH)_2$ and MgO with high surface area porous structures through sol–gel reactions, consisting of hydrolysis reactions (Eqs. 3, 4) and condensation reactions (Eqs. 5, 6) [11–15]. It is known that there are two critical factors affecting the sol–gel products: (1) the amount of water and (2) the pH of the reactions. In the present work, a sol–gel-precipitation method is used to synthesize $Mg(OH)_2$ whiskers on zeolite LTA surfaces, and the whisker morphology is controlled by the sol–gel reaction conditions via manipulation of the amount of water and the pH.

$$Mg(OCH(CH_3)_2)_2 + H_2O \rightleftarrows HOMgOCH(CH_3)_2 + (CH_3)_2CHOH \quad (3)$$

$$HOMgOCH(CH_3)_2 + H_2O \rightleftarrows HOMgOH + (CH_3)_2CHOH \quad (4)$$

$$-MgOCH(CH_3)_2 + -MgOH \rightleftarrows -MgOMg- + (CH_3)_2CHOH \quad (5)$$

$$-MgOH + -MgOH \rightleftarrows -MgOMg- + H_2O. \quad (6)$$

3.1 Effect of magnesium/water ratio and pH on sol–gel $Mg(OH)_2$ morphology

The most important parameter for the sol–gel reaction is the amount of water used, which determines the extent of the hydrolysis and condensation reactions involving the magnesium alkoxide. The stoichiometric amount of water needed to react with magnesium isopropoxide was calculated according to Eq. 7. The amount of magnesium isopropoxide generated by methylmagnesium bromide, as shown in Eq. 1, in each vial is 0.005 mol. One stoichiometric (denoted as 1S) amount of water to react with the magnesium isopropoxide according to Eq. 7 is 0.18 grams.

$$Mg(OCH(CH_3)_2)_2 + 2H_2O \rightleftarrows Mg(OH)_2 + 2(CH_3)_2CHOH. \quad (7)$$

Research showed that hydrolysis reactions of magnesium alkoxides are equilibrium reactions, and the amount of $Mg(OH)_2$ generated depends on the reaction extent [11, 14]. Figure 1 shows the final $Mg(OH)_2$ morphology on a zeolite 5A surface after treatments with different amounts of added water. Treatment with 2S amount of water showed bare zeolite 5A surfaces. This is likely because the hydrolysis reaction (Eq. 7) does not proceed to a large extent under these conditions, and the magnesium isopropoxide remains largely unreacted. The zeolite and sol–gel product mixture was later washed several times using de-ionized water to remove the water soluble reaction products. During the water washing steps, the water soluble magnesium isopropoxide is washed away and little solid forms on the zeolite surfaces. Therefore, during the water washing step, the remaining magnesium isopropoxide does not hydrolyze and form $Mg(OH)_2$ to any appreciable extent. This supposition is consistent with visual observation of the reaction filtrate, which remained clear for an extended period of time and only became cloudy after a few weeks.

When the amount of water is 4S to 6S, $Mg(OH)_2$ solids in the form of short whiskers begin to form on the zeolite surfaces. This is likely because $Mg(OH)_n(OR)_{2-n}$ $(0 < n < 2)$ species are formed as hydrolysis products, and these species are partially insoluble in water, and precipitate onto the zeolite surfaces during the water washing step. As the water amount is increased, more water insoluble hydrolysis product is generated and precipitated onto the zeolite surfaces. As shown in Fig. 1, more plate-like $Mg(OH)_2$ is formed on the zeolite surfaces at 8S water addition. With water addition in excess of 12S, the milky dispersion begins to phase separate into a clear top layer and white, cloudy, bottom layer. It can be concluded that at pH = 7, only short whiskers or flakes of $Mg(OH)_2$ can be generated after addition of varying amounts of water.

It is well known that reaction pH can affect the morphology of sol–gel products. Under acidic conditions, the hydrolysis reactions are promoted, condensation reactions are depressed, and one-dimensional structures, such as nanoparticles, whiskers etc., can be generated [16]. In the well studied sol–gel silicate case, acid-catalyzed hydrolysis with low H_2O:Si ratios produces weakly branched ''polymeric'' sols, whereas base-catalyzed hydrolysis with large H_2O:Si ratios produces highly condensed "particulate" sols. To our knowledge, there has been no relevant prior research on the pH effects on $Mg(OH)_2$ morphologies using the sol–gel method.

In this work, the pH of the water was controlled by making 1 M (pH = 0) and 0.1 M (pH = 1) HCl solutions. The acid solutions were added to the sol dispersion replacing the pure de-ionized water that was used in the base case. The other steps were performed exactly the same.

Figure 2 shows the different morphologies of $Mg(OH)_2$ whiskers on the zeolite surfaces after treatments with different amounts of water of different pH. Longer whiskers were formed in the more acidic environment. The whiskers from treatment at pH = 1 appeared to be short and perpendicular to the zeolite surface. The $Mg(OH)_2$ content was about 3.0 wt% of the total solid, as shown in Table 1. The whiskers from treatment at pH = 0 were longer and

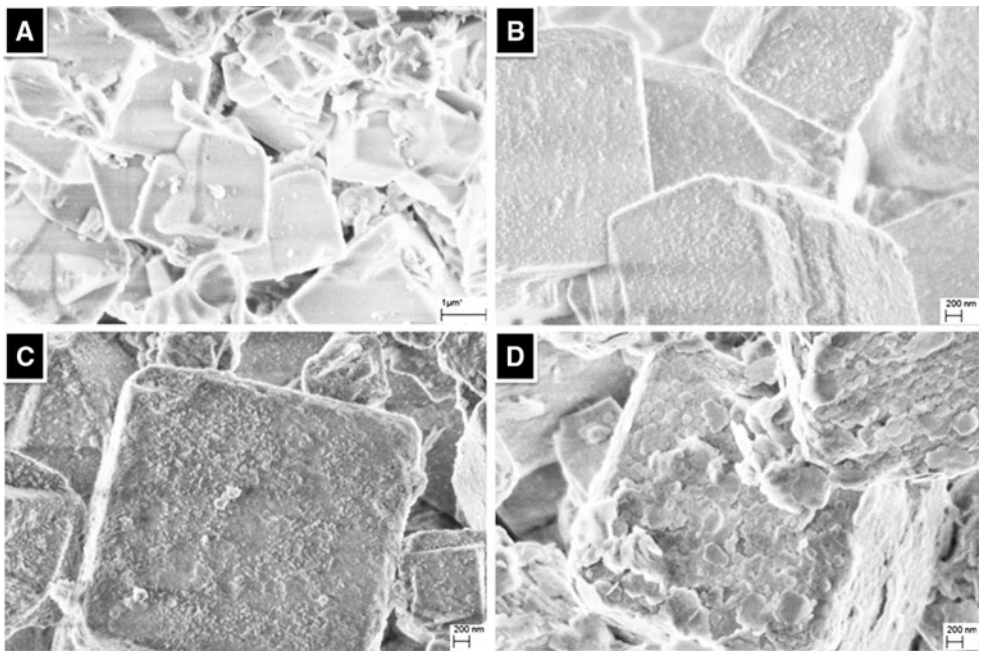

Fig. 1 Different morphologies of $Mg(OH)_2$ formed by adding various amount of water (pH = 7.0): **a**, **b**, **c**, **d** have two, four, six and eight times stoichiometric amount of water

interlocked. The $Mg(OH)_2$ content was about 9 wt% of the total solid, converted from the atomic percentage. These interconnected whisker structures may provide more stable polymer chain entanglement in composite films, as discussed below. The density of the whiskers on the zeolite surface was not evaluated exactly, but there seems to be no dramatic difference between the different treatments as judged by SEM images. The whisker density may be controlled by the density of nucleating sites on the zeolite surface, which is determined by the surface properties of the molecular sieve.

Figure 3 shows the $Mg(OH)_2$ morphologies prepared via addition of more than 6S equivalents of water. In these cases, free $Mg(OH)_2$ particles appear to have formed in solution and then deposited on the zeolite surfaces. This is likely due to homogeneous nucleation at higher hydrolysis levels.

3.2 Magnesium sol formation

Figure 4 shows the images of LTA zeolites at various stages of the $Mg(OH)_2$ functionalization process under a fixed set of conditions (6S H_2O, pH = 0). After quenching the methylmagnesium bromide with isopropanol, it is well known that magnesium bromide and magnesium isopropoxide are formed [8, 9]. Smooth zeolite surfaces were observed after this step. After water addition, an amorphous product on zeolite surface was observed, but no whisker morphology appeared to present on the zeolite surface. After the first water wash, the zeolite surfaces were found to be covered by a thick layer of sol–gel product. After three water washes, only $Mg(OH)_2$ whiskers were observed on the zeolite surfaces.

To better understand the process, the same treatment without addition of zeolite was performed. The products were collected by centrifuge analyzed by XRD (shown in Fig. 5). The magnesium sol, consisting of magnesium bromide and magnesium isopropoxide, showed a clear crystal pattern. After adding water, the crystalline pattern disappeared, consistent with the amorphous morphology suggested in Fig. 4. The hydrolysis and condensation reactions started after water was added, and the intermediate products can associate into polymer-like gels by –Mg–O–Mg– bonding or hydrogen bonding between –Mg–OH groups [11], as shown in Fig. 6. Indeed, after addition of 5S of water, the gel formation was inferred by an increase of viscosity.

Although there should be an equimolar amount of magnesium bromide and magnesium isopropoxide after the isopropanol quenching step, no strong $MgBr_2$ peaks were observed in the XRD pattern after the water addition step. This is probably because the $MgBr_2$ salt is strongly associated into the gel structure shown in Fig. 6, together with water. In this situation, the magnesium gel structures are probably surrounded not only by toluene and isopropanol solvent, but possibly by water and hydrated ions of Mg^{2+}, Br^-. It has been reported that the soluble salts are typically homogeneously dispersed in the sols to give well dispersed

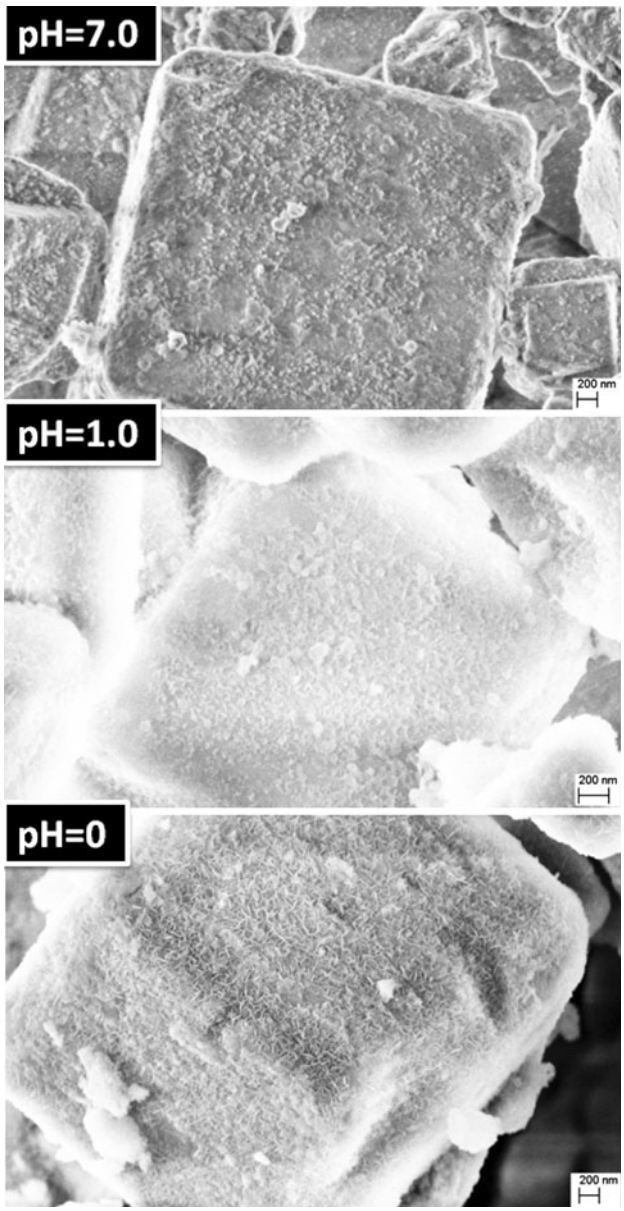

Fig. 2 Different morphologies of $Mg(OH)_2$ formed on 5A surfaces, by adding six times of stoichiometric amount of water at various pHs

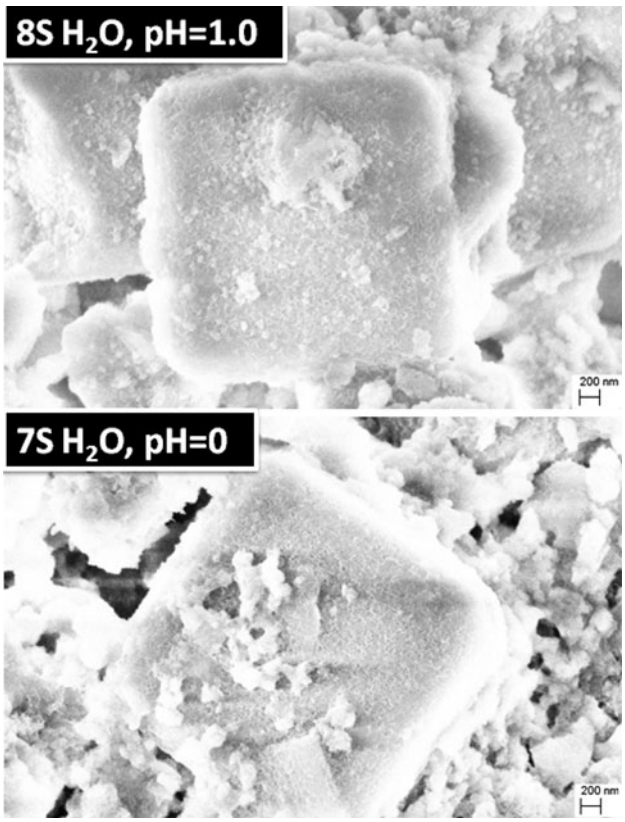

Fig. 3 Independently formed $Mg(OH)_2$ after over amount of water addition

mixture products [16]. It is unknown whether the presence of $MgBr_2$ salts in this work affected the reactions of magnesium isopropoxide and the magnesium hydroxide precipitation process. The XRD pattern of the gel displayed little crystallinity. During the isopropanol wash that was used to remove the toluene from the sol–gel product, the amorphous nature of sol–gel product did not change. When the isopropanol phase was replaced by water, however, the collected sol–gel product showed a clear crystalline pattern associated mainly with $Mg(OH)_2$, and small amount of other impurities, most probably $MgBr_2$. After three of water washes assisted by sonication, only the strong $Mg(OH)_2$ pattern was observed. This agrees with images in Fig. 4 that suggest that most of the $MgBr_2$ and deposited particles were removed after three sonication and water washes. The conductivity of supernatant water for the first three water washes drops from few thousand to about

Table 1 Elemental composition of different 5A particles by EDS measurement

	Atomic percentage %					
	O	Na	Mg	Al	Si	Ca
Bare 5A	54.3	4.9		16.0	16.8	8.1
GT-5A (6S H2O, pH = 7.0)	63.7	3.2	0.4	13.6	13.8	5.4
GT-5A (6S H2O, pH = 1.0)	65.9	2.8	1.1	12.3	12.2	5.4
GT-5A (6S H2O, pH = 0)	61.9	3.5	3.3	13.2	12.4	5.8

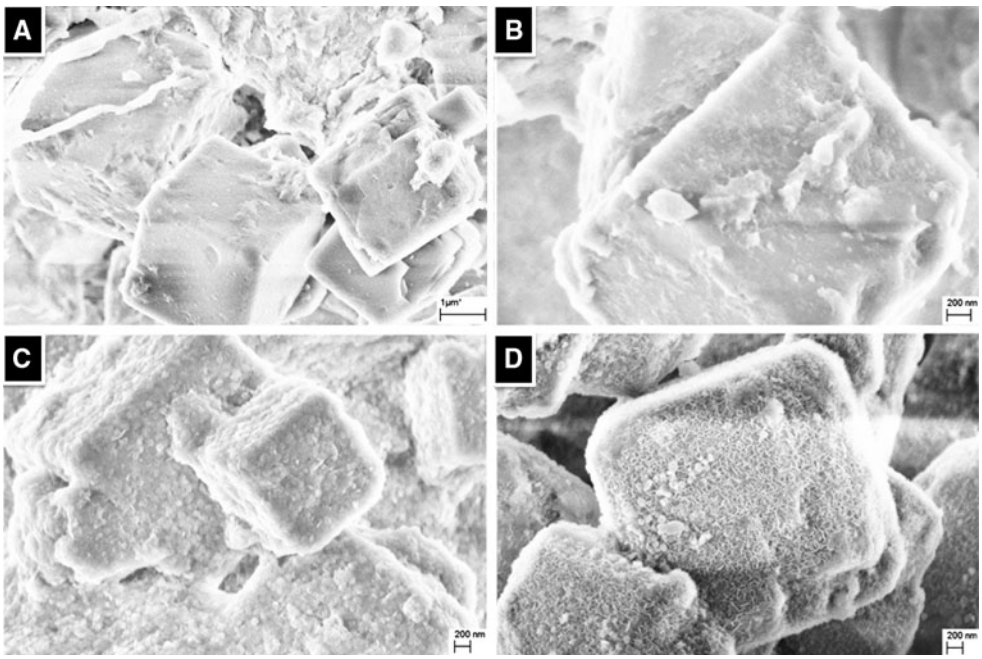

Fig. 4 Morphology development at different stages of treatment (6S H_2O, pH = 0); **a** zeolite in sol–gel precursor (after IPA quenching); **b** zeolite in sol–gel (after water addition); **c** zeolite in precipitated sol–gel (after one water wash); **d**, Zeolite in precipitated sol–gel (after three water wash)

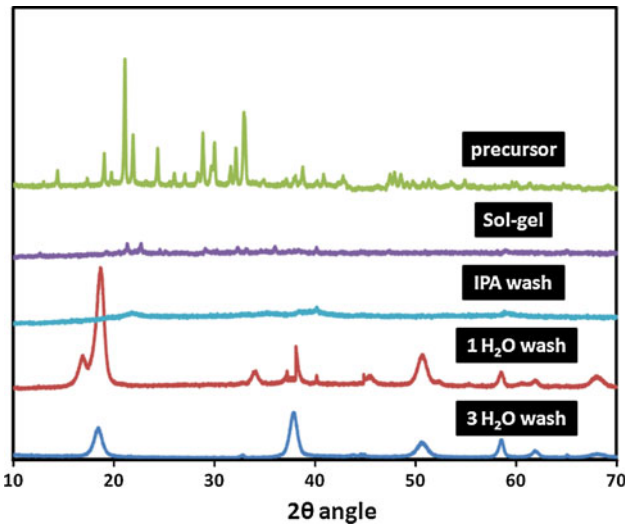

Fig. 5 XRD patterns of sol–gel products at different steps of treatment

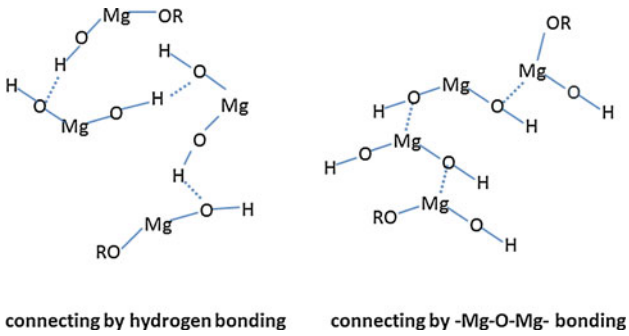

Fig. 6 Examples of polymer like interconnected gel structures formed by hydrolysis and condensation reactions, –OR stands for the unhydrolyzed isopropoxyl group

100 μS m^{-1}, which is probably due to the $MgBr_2$ being washed off.

It can be concluded that the $Mg(OH)_2$ whiskers were formed by a sol–gel-precipitation mechanism, as shown in Fig. 7. The magnesium isopropoxide sol first reacted with water and was transformed into a polymer like amorphous gel. The amorphous gel, made of $Mg(OH)_n(OR)_{2-n}$ then precipitated onto the zeolite surfaces because of its limited solubility in water. The uncompleted hydrolysis reaction was completed and $Mg(OH)_2$ was generated with the abundant water washing.

3.3 $Mg(OH)_2$ precipitation

It appears the gel precipitated preferentially onto the zeolite surfaces, rather than forming homogeneous particles in solution. This suggests the zeolite surface provided heterogeneous nucleating sites. There is typically a high concentration of hydroxyl groups on zeolite surfaces [17]. Methylmagnesium bromide may react with the surface hydroxyl groups as shown in Eq. 8 [18]. Si–O–Mg– bonds can also be generated by condensation reactions, as shown by Eq. 9, between silanol groups and magnesium alkoxides

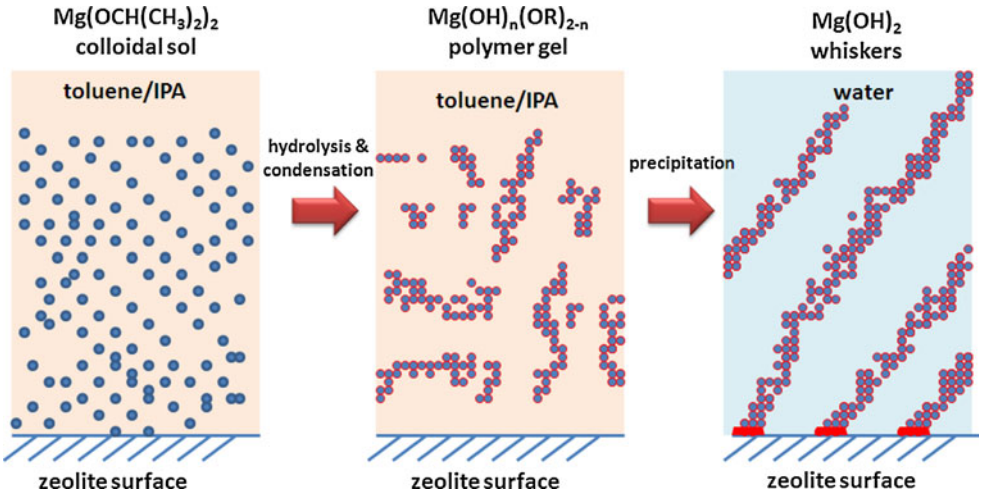

Fig. 7 Morphology evolutions from magnesium alkoxide to magnesium hydroxide, during the sol–gel precipitation steps

[19]. Both of these routes leading to –Si–O–Mg– bonding could provide nucleating sites for $Mg(OH)_2$ precipitation and the potential for covalent bonding between the zeolite and $Mg(OH)_2$ structures. Additional research will be required to elucidate the true mechanism.

$$-\mathrm{Si}-\mathrm{OH} + \mathrm{CH_3MgBr} \rightarrow -\mathrm{Si}-\mathrm{O}-\mathrm{MgBr} + \mathrm{CH_4} \quad (8)$$

$$-\mathrm{Si}-\mathrm{OH} + \mathrm{Mg(OR)(OH)} \rightleftarrows -\mathrm{Si}-\mathrm{O}-\mathrm{Mg}-\mathrm{OH} + \mathrm{ROH}. \quad (9)$$

3.4 Polymer zeolite adhesion enhancement by $Mg(OH)_2$ whiskers

It has been reported that the $Mg(OH)_2$ nanowhiskers on zeolite surfaces may provide molecular scale interlocking interactions with polymer chains and enhance the adhesion between the zeolite and polymer [4]. The adhesion enhancement in this work was evaluated by butane isomer permeation tests using mixed matrix membranes containing treated 5A zeolite particles.

Zeolite 5A has pores that allow n-butane to pass through but totally block the passage of i-butane, i.e., show infinite selectivity for the normal butane isomer [20]. By adding zeolite 5A into polymeric membranes, the butane isomer performance should be enhanced if the zeolite and polymer are properly adhered. To check for the possibility for permeation of n-butane in zeolite 5A before and after the magnesium treatment, sorption measurements were performed and the results are shown in Fig. 8. The n-butane sorption capacity was not changed by treatment under the different conditions. The i-butane adsorbs to essentially no extent in all the samples. Therefore, the micropores of the zeolite were not significantly affected by the acidic water added in the treatments. The ratio between HCl and magnesium isopropoxide was about 1:5, under the 6S water addition conditions, pH = 0. The stability of the zeolite framework was good, as confirmed by the only small change of n-butane sorption capacity in zeolite 5A micropores.

A defective interface (so called 'sieve-in-a-cage' morphology) was formed when bare zeolite 5A was added into the 6FDA-DAM polymer, as shown in Fig. 9. Gas molecules can bypass the zeolite through the defective interfaces. Pinholes can be generated if voids are interconnected in extreme cases. The treated zeolite with the most whisker-like $Mg(OH)_2$ morphology was the sample treated with 6S water addition, at pH = 0 (Fig. 10). In the mixed matrix membrane containing the treated zeolite, the zeolite-polymer interfacial adhesion was improved significantly. The permeation results for these membranes are shown in Table 2. The mixed matrix membrane containing bare 5A had increased n-butane permeability, but the butane isomer selectivity was far lower than that in pure polymer. This is

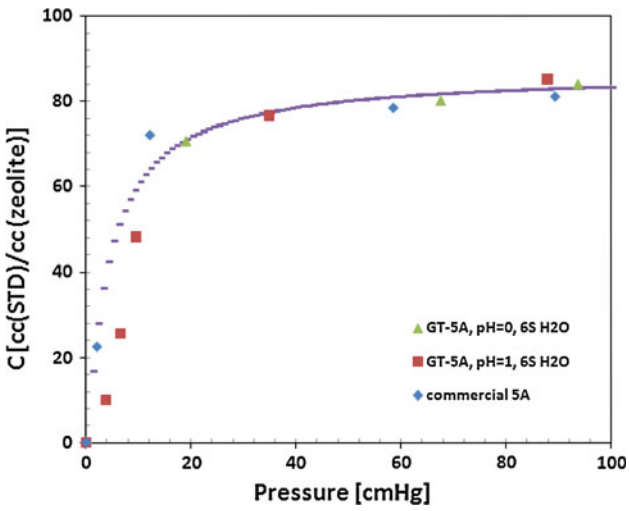

Fig. 8 Sorption isotherm of n-butane in bare and treated 5A samples, at 50 °C. The points are from experimental results, the line is a Langmuir fitting

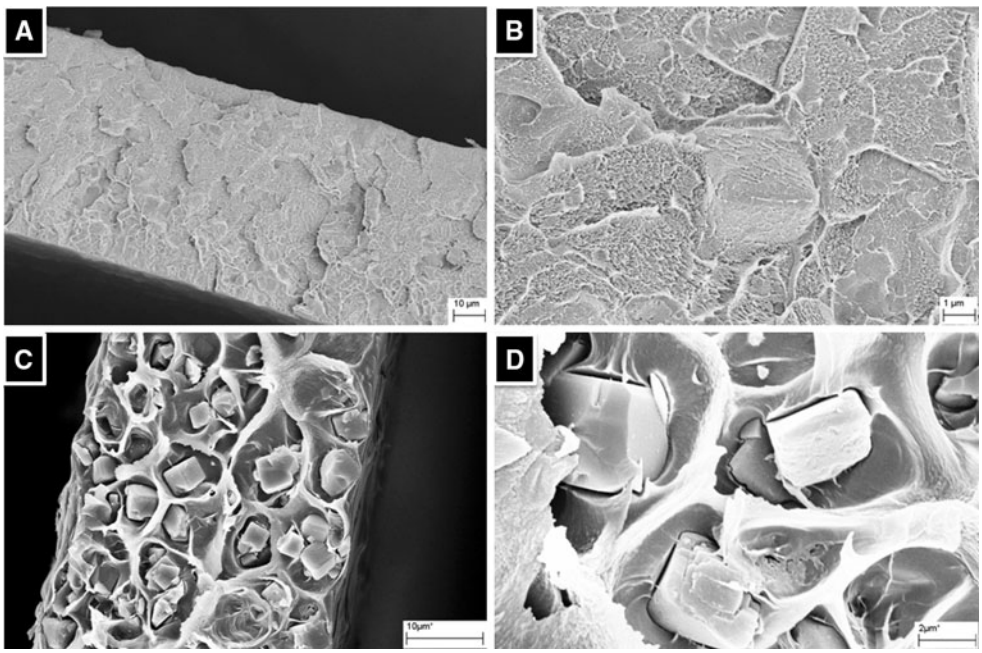

Fig. 9 Cross section of mixed matrix films containing 6FDA-DAM polymer and 25 wt% treated (6S water, pH = 0) 5A (**a**, **b**) and bare 5A (**c**, **d**)

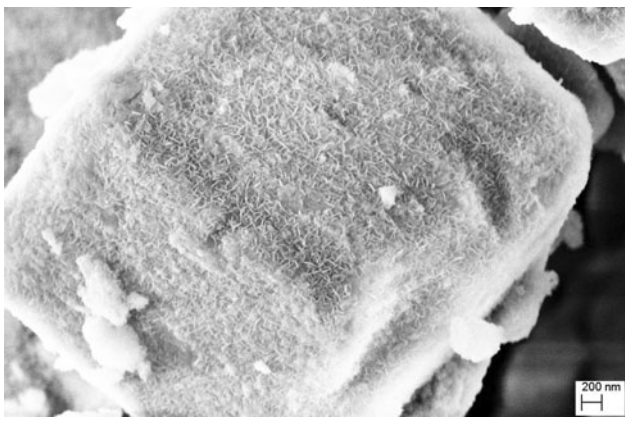

Fig. 10 $Mg(OH)_2$ whiskers formed on 5A surfaces at treatment condition: 6 times of stoichiometric amount of water, pH = 0

Table 2 Permeability and selectivity of C4 s in polymeric and mixed matrix membranes, 100 °C, 25 psi at upstream, GT-5A is done with condition: pH = 0, 6S water

	Permeability nC4 [Barrer]	Selectivity nC4/iC4 [−]
6FDA-DAM	3.2 ± 0.2	21 ± 2
25 wt%-bare 5A-6FDA-DAM	4.5 ± 0.3	2.5 ± 0.3
25 wt%-GT-5A -6FDA-DAM	3.3 ± 0.2	25 ± 2

possibly due to pinholes generated by the defective interfaces. In the mixed matrix membrane containing treated zeolite 5A, the butane isomer selectivity increased about 20% due to the addition of i-butane blocking 5A particles. The n-butane permeability was not increased because the rates of n-butane diffusion were about the same in the 6FDA-DAM polymer and zeolite 5A, which will be discussed in a separate paper. The selectivity enhancement in the mixed matrix membrane confirms the good adhesion suggested by the SEM images.

4 Conclusion

The three step sol–gel-precipitation developed based on knowledge of the probable mechanism of $Mg(OH)_2$ formation on the zeolite surface successfully resulted in magnesium hydroxide nanowhisker functionalized zeolite 5A. Magnesium isopropoxide, the precursor for the sol–gel reaction, was formed by quenching the methylmagnesium bromide with isopropanol. After controlled water addition, the hydrolysis and condensation reactions started, and gelation occurred. The amorphous polymer-like $Mg(OH)_n(OR)_{2-n}$ then precipitates out of the water solution and onto the zeolite surfaces, because of its limited solubility. The amount of added water determined the extent of the hydrolysis reactions, and the composition of $Mg(OH)_n(OR)_{2-n}$ formed. When water was not added, $Mg(OH)_n(OR)_{2-n}$ was largely $Mg(OR)_2$, and nothing was formed on the zeolite surface, because the water soluble $Mg(OR)_2$ was washed away. When more water was added, $Mg(OH)_n(OR)_{2-n}$ trends closer to $Mg(OH)_2$ in composition and precipitate out of water solution. The amount of $Mg(OH)_2$ formed was controlled by the hydrolysis extent via the amount of water added. The addition HCl affected the

hydrolysis and condensation reactions, and the structure of polymer gels formed. The whisker morphology was formed using acidic water for the sol–gel reactions. The formation of $Mg(OH)_2$ whiskers on the zeolite surfaces showed little effect on the microporosity of the zeolite 5A. The $Mg(OH)_2$ whiskers on the zeolite surfaces helped the interfacial adhesion between the zeolite and polymer, possibly by providing more surface area for entanglement of the polymer chains.

Acknowledgment The authors want to thank ExxonMobil and the King Abdullah University of Science and Technology (Award No. KUS-I1-011-21) for sponsoring this research. We are also grateful to Harry Deckman, Edward Corcoran and Ben McCool for helpful suggestions.

References

1. Koros WJ, Mahajan R (2000) J Membr Sci 175:181–196
2. Mahajan R, Burns R, Schaeffer R, Koros WJ (2000) J Appl Polym Sci 86:881–890
3. Moore T, Koros WJ (2005) J Mol Struct 739:87–98
4. Shu S, Husain S, Koros WJ (2007) Chem Mater 19:4000–4006
5. Shu S, Husain S, Koros WJ (2007) J Phys Chem C 111:652–657
6. Husain S, Koros WJ (2007) J Membr Sci 288:195–207
7. Shu S, Husain S, Koros WJ (2007) Ind Eng Chem Res 46:767–772
8. Fieser LF (1956) Organic chemistry. Reinhold, New York
9. Bruice PY (2007) Organic chemistry. Pearson Prentice Hall, New Jersey
10. Liu J, Bae TH, Qiu W, Nair S, Jones CW, Chance RR, Koros WJ (2009) J Membr Sci 343:157–163
11. Diao Y, Walawender WP, Sorensen CM, Klabunde KJ, Ricker T (2002) Chem Mater 14:362–368
12. Utamapanya S, Klabunde KJ, Schlup JR (1991) Chem Mater 3:175–181
13. Stengl V, Bakardjieva S, Maikova M, Bezdi P, Subrt J (2003) Mater Lett 57:3998–4003
14. Lopez T, Garcia-Cruz I, Gomez R (1991) J Catal 127:75–85
15. Francis LF (1997) Mater Manuf Process 12:963–1015
16. Brinker CJ (1990) Sol-gel science. Academic Press, Inc., New York
17. Ward JW (1967) J Catal 9:225–236
18. Sato M, Kanbayashi T, Kobayashi N, Shima Y (1967) J Catal 7:342–351
19. Yoon JG (1995) Appl Phys Lett 66:2661–2663
20. Karger J (1992) Diffusion in zeolites. Wiley, New York